

{1,1'-(Dimethylsilylene)bis[methanechalcogenolato]}diiron Complexes [2Fe2E(Si)] (E = S, Se, Te) – [FeFe] Hydrogenase Models

by Ulf-Peter Apfel^{a)}, Helmar Görls^{a)}, Greg A. N. Felton^{c)}, Dennis H. Evans^{*d)}, Richard S. Glass^{*c)},
Dennis L. Lichtenberger^{*c)}, and Wolfgang Weigand^{*a)}

^{a)} Institut für Anorganische und Analytische Chemie, Friedrich-Schiller-Universität Jena,
Humboldtstrasse 8, D-07743 Jena (e-mail: wolfgang.weigand@uni-jena.de)

^{b)} Massachusetts Institute of Technology, 77 Massachusetts Avenue, Cambridge, MA, 02139, USA

^{c)} Department of Chemistry and Biochemistry, The University of Arizona, Tucson, AZ, 85721, USA

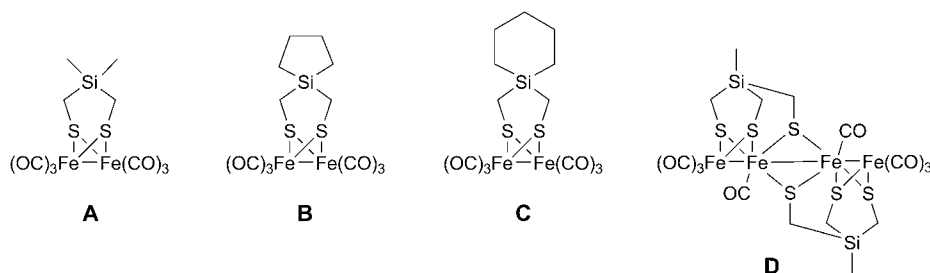
^{d)} Department of Chemistry, Purdue University, West Lafayette, IN, 47907, USA

Dedicated to Professor *Dieter Seebach* on the occasion of his 75th birthday

(Bis-selenolato) and (bis-telluroolato)diiron complexes [2Fe2E(Si)] were prepared and compared with the known (bis-thiolato)diiron complex **A** to assess their ability to produce hydrogen from protons. Treatment of [Fe₃(CO)₁₂] with 4,4-dimethyl-1,2,4-diselenasilolane (**1**) in boiling toluene afforded hexacarbonyl{μ-[[1,1'-(dimethylsilylene)bis[methaneselenolato-κSe : κSe]](2 –)}]diiron(Fe–Fe) (**2**). The analog bis-telluroolato complex hexacarbonyl{μ-[[1,1'-(dimethylsilylene)bis[methanetelluroolato-κTe : κTe]](2 –)}]diiron(Fe–Fe) (**3**) was obtained by treatment of [Fe₃(CO)₁₂] with dimethylbis(tellurocyanatomethyl)dimethylsilane, which was prepared *in situ*. All compounds were characterized by NMR, IR spectroscopy, mass spectrometry, elemental analysis and single-crystal X-ray analysis. The electrocatalytic properties of the [2Fe2X(Si)] (X = S, Se, Te) model complexes **A**, **1**, and **2** towards hydrogen formation were evaluated.

Introduction. – Since the structure of the active site of the [FeFe] hydrogenase has been reported [1], finding a suitable model with comparable properties, *i.e.*, high turnover rates with low overpotential for the reversible reduction of protons to molecular hydrogen, is still a challenge. Recent progress in this topic was achieved by *Darensbourg* and co-workers concerning the investigations of the ‘rotated’ geometry on [2Fe2S] model complexes [2] and by *Barton* and *Rauchfuss* discerning the role of phosphine ligands in directing protons to a bridging or terminal site [3]. Beside the direct protonation of the Fe centers, experiments and calculations pointed out a possible addition of a proton to the bridgehead S-atoms [4]. An experimental proof of these calculations was displayed by silicon containing [2Fe2S] models **A–D** (*Fig. 1*) [5].

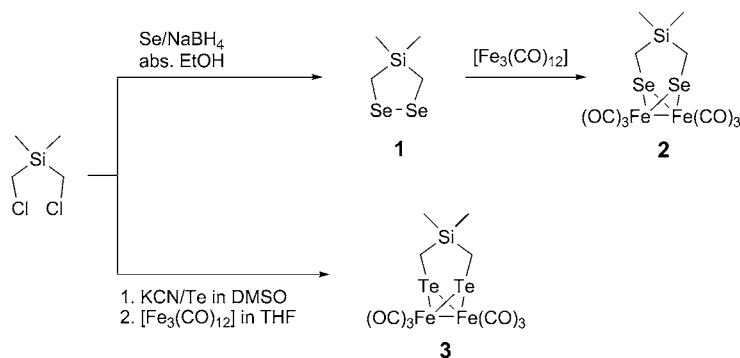
Recent investigations of our group suggested that in contrast to the propane-1,3-dithiolato (pdt) iron complexes [6], an increase of electron density on the S-atoms by interaction of the σ(Si–C) and 3p(S) orbitals can be assumed. Similar interactions were found for comparable tin complexes, described by *Glass* and co-workers [7]. During electrochemical investigations, protonation of the thiolato S-atoms was observed, and a subsequent proton shift to the iron core suggested. More recently, investigations on hexacarbonyl(2-oxaspiro[3.4]octane-6,7-dichalcogenolato)diiron complexes revealed diminished activity towards hydrogen production and negatively shifted potentials for


 Fig. 1. $[Fe_2S_2Si]$ Model complexes

the one-electron reduction of the $[FeFe]$ cluster upon chalcogen exchange, according to $S > Se > Te$ [8]. Inspired by the unique chemistry of silicon-containing $[FeFe]$ -hydrogenase model complexes and the results on chalcogen exchange, 1,1'-(dimethylsilylene)bis[methanechalcogenolato] complexes **2** and **3** were synthesized. The spectroscopic and structural features as well as the electrocatalytic properties were investigated and compared with the related S-containing complex **A** to investigate their capability to act as proton reduction catalysts.

Results and Discussion. – Recently, the synthesis of bis(mercaptomethyl)dimethylsilane and its respective $[2Fe_2S]$ complex was described [5][9]. However, this synthetic procedure had to be modified to afford the analogous selenium and tellurium complexes. An intensive literature research showed that *Block* and co-workers had already established the syntheses of dimethylbis(selenomethyl)silane and dimethylbis(telluromethyl)silane [9].

In contrast to *Block* and co-workers, we favored the reaction of the selenium or tellurium precursors from easily accessible bis(chloromethyl)dimethylsilane instead of bis(iodomethyl)dimethylsilane as starting material. Upon reaction of bis(chloromethyl)dimethylsilane with sodium diselenide, which was prepared *in situ* from selenium and sodium borohydride in absolute ethanol, 4,4-dimethyl-1,2,4-diselenasilolane (= 4,4-dimethyl-1,2-diselena-4-silacyclopentane; **1**) was obtained in 28% yield as a red solid (*Scheme*).

 Scheme. Synthesis of Model Complexes **2** and **3**


Reaction of compound **1** with $[\text{Fe}_3(\text{CO})_{12}]$ provided hexacarbonyl $\{\mu\text{-}[[1,1'\text{-}(\text{dimethylsilylene})\text{bis}[\text{methaneselenolato-}\kappa\text{Se}:\kappa\text{Se}]](2-)]\}$ diiron(Fe-Fe) (**2**) in moderate yield (66%). ^1H -, $^{13}\text{C}\{^1\text{H}\}$ -, and $^{77}\text{Se}\{^1\text{H}\}$ -NMR spectra and the mass spectrum (MS) showing the M^+ peak at m/z 526, followed by stepwise loss of six CO fragments, revealed the proposed structure. Evaporation of a solution of **2** in pentane afforded crystals suitable for single-crystal X-ray structure determination, as depicted in Fig. 2. In contrast to the selenium compound, the synthesis of hexacarbonyl $\{\mu\text{-}[[1,1'\text{-}(\text{dimethylsilylene})\text{bis}[\text{methanetelluroolato-}\kappa\text{Te}:\kappa\text{Te}]](2-)]\}$ diiron(Fe-Fe) (**3**) followed a different route, as the bis-telluroolato compound turned out to be elusive. Therefore, bis(chloromethyl)dimethylsilane was treated with a twofold excess of potassium tellurocyanate, freshly prepared by heating tellurium and potassium cyanide in refluxing dimethyl sulfoxide [10]. The *in situ* prepared dimethylbis(tellurocyanatomethylo)silane was not isolated but immediately added to a solution of $[\text{Fe}_3(\text{CO})_{12}]$ dissolved in THF. Subsequent heating of this solution under reflux conditions, followed by exhaustive extraction with hexane as well as chromatographic purification, afforded a small amount of compound **3** (9%) as orange powder. NMR Investigations (^1H , $^{13}\text{C}\{^1\text{H}\}$) suggested compound **3**, which was additionally confirmed by the M^+ peak present at m/z 624 in its MS. Single crystals suitable for structure determination were obtained by slow evaporation of a solution of **3** in pentane (Fig. 2).

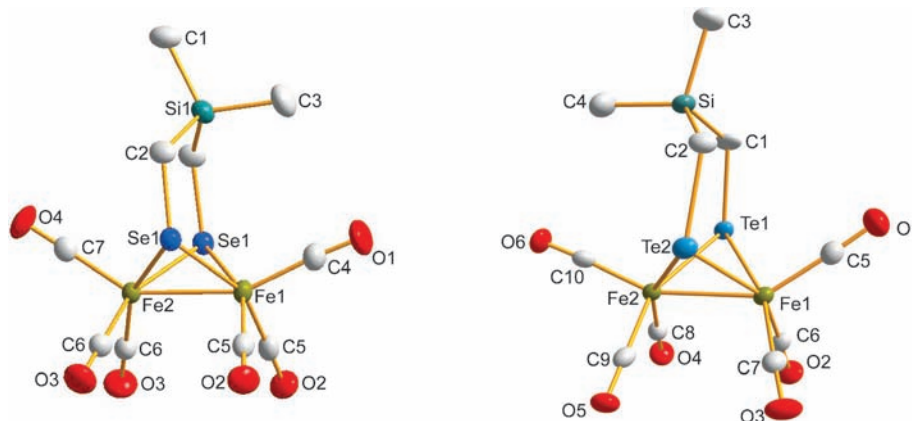


Fig. 2. Molecular structure of **2** (left) and **3** (right) in the crystal (probability level of displacement ellipsoids 50%)

Since the CO group is very sensitive towards changes of the electron density on the Fe-centers, the $^{13}\text{C}\{^1\text{H}\}$ -NMR signals and the CO vibrations give important insight to the electronic influence of the Se- and Te-atoms [11]. Comparing compounds **1**, **2**, and **3**, the CO vibrations shift from 2074 cm^{-1} for the S-compound **1** to 2065 cm^{-1} for the Se-compound **2**, to 2054 cm^{-1} for the Te-compound **3**. This shift to lower wave numbers can be best explained by the higher electron density directed to the iron Fe-centers induced by the heavier Se- and Te-homologues [8d]. This tendency is also apparent in the $^{13}\text{C}\{^1\text{H}\}$ -NMR spectra. A continuous deshielding of the CO groups and hence a shift to lower field of their signal is observable within the homologous row S ($\delta(\text{C})$ 207.5), Se ($\delta(\text{C})$ 208.4), and Te ($\delta(\text{C})$ 210.5) [11]. Another significant influence

of the exchange of S by Se or Te is detectable for the E–CH₂–Si (E = S, Se, Te) ¹³C-NMR chemical shifts. Whereas S-compound **A** exhibits this signal at $\delta(\text{C})$ 5.9, the Se-derivative **2** reveals it at $\delta(\text{C})$ –5.1; this shift is even more pronounced for the related Te-compound **3** for which this resonance appears at $\delta(\text{C})$ –26.6. This distinctive high-field shift is only explainable by the heavy-atom effect [12].

As the spectroscopic differences strongly deviate, one may assume that the structural properties should differ, but this could only be confirmed for the Fe–Fe bond distance. As compound **A** reveals a distance of 252.16(6) pm, compound **2** shows a slightly longer Fe–Fe bond with a distance of 254.99(6) pm (*Table 1*). The Fe–Fe bond of compound **3** reveals a significantly increased distance of 261.53(8) pm. By all means, this phenomenon was expected as the atomic radii of the higher homologues are enlarged. Collectively, all three compounds exhibit the typical [2Fe2S] ‘butterfly’ arrangement and bear six CO groups as seen in many similar [2Fe2S] complexes [13]. Although, a significant IR change of the CO vibrations could be observed, the Fe–C(O) and C=O distances remained unchanged. As already recorded for compound **A**, wide bonding angles E–C–Si were observed for **2** and **3**. This might suggest that also for compounds **2** and **3**, an increased basicity of the chalcogenolato atoms E (E = S, Se, Te) should be expected as a result of an effective overlap according to $\sigma(\text{C–Si}) \rightarrow n_{\text{p}}(\text{E})$.

Table 1. Selected Bond Distances and Angles for Compounds **2** and **3**

Bond lengths [pm]			Bond angles [°]		
	2	3		2	3
Fe(1)–Fe(2)	254.99(6)	261.53(8)	Fe(1)–Se(1)/Te(1)–Fe(2)	64.817(15)	61.777(18)
Fe(1)–Se(1)/Te(1)	238.03(4)	255.70(6)	Te(1)–C(1)–Si	–	121.7(2)
Fe(2)–Se(1)/Te(2)	237.73(4)	254.14(5)	Se(1)/Te(2)–C(2)–Si	121.55(15)	119.4(2)
Te(1)–C(1)	–	216.0(4)	C(1)–Si–C(2)	107.58(12)	106.70(19)
Se(1)/Te(2)–C(2)	195.8(3)	216.9(4)	C(1)–Si–C(3)	109.8(2)	107.8(2)
Si(1)–C(1)	186.9(4)	186.7(4)	C(1)–Si–C(4)	–	113.8(2)
Si(1)–C(2)	187.1(3)	185.8(4)			
Si(1)–C(3)	185.8(5)	187.5(5)			
Fe–C(O) _{average}	179.7	178.5			
C=O _{average}	113.7	114.5			

Electrochemistry. Cyclic voltammetry of **2** and **3** studied in MeCN in the presence of 0.100M (Bu₄N)PF₆ at 25° and with a glassy carbon working electrode revealed a partially reversible reduction with peak potentials as shown in *Table 2*. By comparison with compound **A**, which is known to undergo a two-electron reduction [5], the reductions of **2** and **3** also appear to be two-electron processes, at least at low scan rates. A slight degree of reversibility is seen for the reduction of each compound, and this is more pronounced at rapid scan rates, more so under CO compared to Ar. The reduction potentials for **2** and **3** are identical within experimental error showing that the change from Se to Te hardly affects the LUMO energy.

The oxidation potentials (also shown in *Table 2*) are somewhat larger for the Se-containing complex **2** than for the Te-compound **3**, and they are still larger for the bis-thiolato complex **A**. These oxidations are all irreversible, and the peak currents

Table 2. Peak Potentials for Reduction ($E_{p,c}$) and Oxidation ($E_{p,a}$) of **A**, **2**, and **3** vs. the Standard Potential of Ferrocene/Ferrocenium^{a)}

	Gas	$E_{p,c}$ [V]	$E_{p,a}$ [V]
A [5]	Ar	-1.52	+0.89
2	Ar	-1.51	+0.70
	CO	-1.51	+0.69
3	Ar	-1.51	+0.62
	CO	-1.52	+0.65

^{a)} Scan rate = 0.100 V/s. MeCN as solvent with 0.100M (Bu₄N)PF₆ as electrolyte. *T* 298 K.

correspond to about a two-electron overall reaction under CO and up to an overall four-electron process under Ar.

The complexes **2** and **3** were tested with respect to their ability to catalyze the reduction of protons from a weak acid, acetic acid, under the same conditions as used for the voltammetric studies of the complexes alone. Compound **2**, under Ar, showed a clear catalytic current near -2.0 V vs. ferrocene/ferrocenium that reached *ca.* 300 μ A at 50 mM acetic acid (1 mM **2**, 0.100 V/s). Further increases in current seen at more negative potentials are likely due in part to direct reduction of acetic acid at the glassy carbon working electrode. Interestingly, this 300 μ A catalytic current was reduced to about 80 μ A when the purge gas was changed from Ar to CO. With **3** under Ar, a similar catalytic current was seen near -1.9 V but its magnitude was only *ca.* 150 μ A, falling to *ca.* 70 μ A under CO. These catalytic currents are modest and are similar to what is seen with related complexes [14].

Conclusions. – The present study revealed a novel series of bis-chalcogenolatodiron complexes containing a Si-atom in the bridging bis-chalcogenolato ligand. Whereas complex **A** was exhaustively investigated as a model complex of the [FeFe] hydrogenase active site, complexes containing Se or Te in the bidentate ligand are rare, and even fewer examples are known sharing the same backbone. Therefore, complexes **2** and **3** allow a direct comparison between homologous bis-chalcogenolato ligands and give insight into the importance of the dithiolato cofactor in [FeFe] hydrogenases. ¹H- and ¹³C-NMR spectroscopic as well as IR spectroscopic studies revealed the different electronic nature of the complexes induced by the replacement of S by Se or Te. A consistent trend could be observed when S was replaced by its higher homologues, namely the increase of electron density on the Fe-atoms. This trend, however, was not observable in the structural parameters of all three compounds, and unexpectedly, no differences could be observed for the electrochemical reduction potential of complexes **A**, **2**, and **3**, suggesting similar energies for the LUMO orbitals. For all complexes, hydrogen formation on electrochemical reduction could be observed in the presence of acetic acid. The activity towards hydrogen formation, however, was highly dependent on the nature of the chalcogen atoms. Whereas the S-containing complex **A** revealed high activity, the Se-containing complex **2** showed decreased activity towards hydrogen formation. Even less activity was observed for the Te-containing complex **3**. Despite the expected trend that increasing the electron density on the Fe-centers would lead to an

increased activity due to rapid protonation of the Fe-center as observed for CO substitution by phosphines, substitution of S by its higher homologues in the ligand does not support this assumption. Apparently, the structural changes in the [2Fe2S] site with increasing size of the E-atom from S to Se to Te outweigh the effects of the increasing donor ability of the E-atom and the increasing electron density on the Fe centers on the rate of catalysis. Previously, we reported that the increase in the Fe–Fe distance with increasing chalcogen size decreases the ability of the complex to form the structure with a ‘rotated’ Fe(CO)₃ group and a vacant coordination site for protonation [8d]. This suggests that the S-atoms are intimately involved in the mechanism for proton reduction, such that both their geometric and their electronic structural features are pivotal for the activity of the complex.

U.-P. A. is thankful for a financial support by the *Studienstiftung des deutschen Volkes* and the *Alexander von Humboldt Foundation*. *D. H. E.*, *R. S. G.*, and *D. L. L.* gratefully acknowledge support of this research by the *NSF* (Grant Nos. 0527003, 1111570, and 1111718).

Experimental Part

General. All syntheses were carried out under dry N₂ or Ar. The org. solvents used were dried and purified according to standard procedures and stored under dry N₂ or Ar. Chemicals were used as received from *Fluka* and *Acros* without further purification. TLC: *Merck* silica gel 60 *F*₂₅₄ plates; detection under UV light at 254 nm. Flash chromatography (FC): *Fluka* silica gel 60. A *Büchi GKR-51* apparatus was used for the bulb-to-bulb distillations. IR-Spectra: *Perkin-Elmer 2000 FT-IR*, in cm⁻¹. ¹H-, ¹³C{¹H}-, and ⁷⁷Se{¹H}-NMR Spectra: *Bruker-200* MHz spectrometer; at 200 (¹H), 50 (¹³C), and 76 MHz (⁷⁷Se); at 23° in CDCl₃; chemical shifts δ in ppm rel. to internal CHCl₃ (δ (H) 7.24; CDCl₃), CDCl₃ (δ (C) 77.0; CDCl₃), or SeO₂ in D₂O, δ (Se) rel. to neat Me₂Se (δ (Me₂Se) = δ (SeO₂) + 1302.6) [15]. MS: *SSQ 710 Finnigan MAT* spectrometer, DEI = desorption electro ionization; in *m/z*.

Electrochemistry. Apparatus and procedures for electrochemistry were the same as described in our earlier paper [8d], with the exception that either Ar or CO was used to purge the cell of dissolved air.

4,4-Dimethyl-1,2,4-diselenasilolane (1). According to [9], but instead of bis(iodomethyl)dimethylsilane, bis(chloromethyl)dimethylsilane was used: To selenium (353 mg, 4.47 mmol) in EtOH (20 ml), sodium borohydride (118 mg, 3.2 mmol) was added at 0°. After 1 h stirring under reflux conditions, bis(chloromethyl)dimethylsilane (500 mg, 3.2 mmol) was added and stirred for 1 h at r.t. Addition of H₂O (20 ml), extraction with CH₂Cl₂, drying (Na₂SO₄), and concentration afforded a crude red oily product which was purified by FC (CH₂Cl₂/hexane 1:5): 220 mg (28%) of **1**. Red solid. ¹H-NMR (CDCl₃): 0.21 (s, 2 CH₃); 2.32 (s, 2 CH₂). ¹³C-NMR (CDCl₃): -1.6 (CH₃); 14.3 (CH₂). ⁷⁷Se{¹H}-NMR (CDCl₃): 319.8. DEI-MS: 246 (*M*⁺).

Hexacarbonyl[μ -{[1,1'-(dimethylsilylene)bis[methanethiolato- κ S : κ S]](2-)}]diiron(Fe-Fe) (A). was prepared according to [5].

Hexacarbonyl[μ -{[1,1'-(dimethylsilylene)bis[methaneselenolato- κ S : κ S]](2-)}]diiron(Fe-Fe) (2). A soln. of **1** (92 mg, 0.37 mmol) and [Fe₃(CO)₁₂] (190 mg, 0.37 mmol) in toluene (40 ml) was stirred under reflux for 1.5 h. Evaporation and filtration through a silica gel pad with CH₂Cl₂/hexane 1:5 afforded 128 mg (66%) of **2**. Red crystalline product. IR (KBr): 2959*m*, 2922*m*, 2897*m*, 2065*vs*, 2021*vs*, 1986*vs*, 1405*m*, 1367*m*, 1253*s*, 1096*s*. ¹H-NMR (CDCl₃): 0.09 (s, 2 CH₃); 1.35 (s, 2 CH₂). ¹³C-NMR (CDCl₃): -5.6 (CH₂), -1.0 (CH₃); 208.4 (CO). ⁷⁷Se{¹H}-NMR (CDCl₃): 170.1. DEI-MS: 526 (*M*⁺), 498 ([*M* - CO]⁺), 470 ([*M* - 2CO]⁺), 442 ([*M* - 3CO]⁺), 414 ([*M* - 4CO]⁺), 386 ([*M* - 5CO]⁺), 358 ([*M* - 6CO]⁺). Anal. calc. for C₁₀H₁₀Fe₂O₆Se₂Si · 0.1 hexane: C 23.91, H 2.16; found: C 23.7, H 2.4.

Hexacarbonyl[μ -{[1,1'-(dimethylsilene)bis[methanetellurolato- κ Te : κ Te]](2-)}]diiron(Fe-Fe) (3). Tellurium (246 mg, 1.92 mmol) and KCN (125 mg, 1.92 mmol) were dissolved in dimethyl sulfoxide (20 ml) and refluxed for 1 h. After cooling to r.t., bis(chloromethyl)dimethylsilane (150 mg, 0.96 mmol) was added, and the soln. was stirred overnight. Subsequently, a soln. of [Fe₃(CO)₁₂] (484 mg, 0.96 mmol)

in THF (20 ml) was added, and the mixture was stirred under reflux for 1 h and then extracted with hexane (until the hexane fraction remained colorless). Evaporation followed by FC (hexane) yielded 51 mg (9%) of **3**. Orange solid. IR (KBr): 2953m, 2922m, 2851m, 2051vs, 2012vs, 1987vs, 1958vs, 1949vs, 1463m, 1377m, 1260m. ¹H-NMR (CDCl₃): 0.08 (s, 2 CH₃); 1.34 (s, 2 CH₃). ¹³C-NMR (CDCl₃): –26.6 (CH₂), –2.1 (CH₃); 210.5 (CO). DEI-MS: 624 (M⁺), 596 ([M – CO]⁺), 568 ([M – 2CO]⁺), 484 ([M – 5CO]⁺), 454 ([M – 6CO]⁺). Anal. calc. for C₁₀H₁₀Fe₂O₆SiTe₂·hexane: C 27.17, H 3.42; found: C 27.53, H 2.93.

*Crystal Structure Determination*¹⁾. The intensity data were collected with a *Nonius-KappaCCD* diffractometer and graphite-monochromated MoK_α radiation. Data were corrected for *Lorentz* and polarization effects but not for absorption [16][17].

The structure was solved by direct methods (SHELXS [18]) and refined by full-matrix least squares techniques against F_o² (SHELXL-97 [18]). All H-atoms were included at calculated positions with fixed thermal parameters. All non-H-atoms were refined anisotropically [18].

Crystal Data of 2: C₁₀H₁₀Fe₂O₆Se₂Si, M_r 523.89; red-brown prism, size 0.06 × 0.06 × 0.03 mm; monoclinic, space group P2₁/m; a = 8.9119(2), b = 10.5919(4), c = 9.7785(3) Å, β = 113.103(2)°, V = 849.00(5) Å³; T = 90°, Z = 2, ρ_{calc.} = 2.049 g cm^{–3}, μ(MoK_α) = 60.84 cm^{–1}; F(000) = 504, 8513 reflections in h(–11/11), k(–13/11), l(–12/11), measured in the range 2.48° ≤ θ ≤ 27.45°, completeness θ_{max} = 99.7%, 2041 independent reflections, R_{int} = 0.0911, 1849 reflections with F_o > 4σ(F_o), 110 parameters, 0 restraints, R_{obs}¹ = 0.0330, wR_{obs}² = 0.0813, R_{all}¹ = 0.0383, wR_{all}² = 0.0844, goodness-of-fit = 1.093, largest difference peak and hole: 0.944/–1.227 e Å^{–3}.

Crystal Data of 3: C₁₀H₁₀Fe₂O₆SiTe₂, M_r 621.17; red-brown prism, size 0.06 × 0.06 × 0.04 mm; triclinic, space group P $\bar{1}$; a = 7.5195(2), b = 9.2175(4), c = 13.4613(5) Å, α = 104.661(2), β = 102.783(2), γ = 98.023(2)°, V = 861.15(5) Å³, T = 90°, Z = 2, ρ_{calc.} = 2.396 g cm^{–3}, μ(MoK_α) = 50.92 cm^{–1}; F(000) = 576, 9543 reflections in h(–9/9), k(–11/10), l(–16/17), measured in the range 1.62° ≤ θ ≤ 27.45°, completeness θ_{max} = 99.3%, 3918 independent reflections, R_{int} = 0.0622, 3454 reflections with F_o > 4σ(F_o), 192 parameters, 0 restraints, R_{obs}¹ = 0.0340, wR_{obs}² = 0.0865, R_{all}¹ = 0.0431, wR_{all}² = 0.0911; goodness-of-fit = 1.053; largest difference peak and hole: 1.349/–1.822 e Å^{–3}.

REFERENCES

- [1] J. W. Peters, W. N. Lanzilotta, B. J. Lemon, L. C. Seefeldt, *Science (Washington, DC, U.S.)* **1998**, 282, 1853; Y. Nicolet, C. Piras, P. Legrand, C. E. Hatchikian, J. C. Fontecilla-Camps, *Structure* **1999**, 7, 13.
- [2] M. L. Singleton, N. Bhuvanesh, J. H. Reibenspies, M. Y. Darensbourg, *Angew. Chem., Int. Ed.* **2008**, 47, 9492.
- [3] B. E. Barton, T. B. Rauchfuss, *Inorg. Chem.* **2008**, 47, 2261.
- [4] J.-F. Capon, S. Ezzaher, F. Gloaguen, F. Y. Pétillon, P. Schollhammer, J. Talarmin, *Chem. – Eur. J.* **2008**, 14, 1954; C. Greco, G. Zampella, L. Bertini, M. Bruschi, P. Fantucci, L. De Gioia, *Inorg. Chem.* **2007**, 46, 108.
- [5] U.-P. Apfel, D. Troegel, Y. Halpin, S. Tschierlei, U. Uhlemann, H. Görls, M. Schmitt, J. Popp, P. Dunne, M. Venkatesan, M. Coey, M. Rudolph, J. G. Vos, R. Tacke, W. Weigand, *Inorg. Chem.* **2010**, 49, 10117.
- [6] J. W. Tye, M. Y. Darensbourg, M. B. Hall, *J. Mol. Struct.: THEOCHEM* **2006**, 771, 123;
- [7] R. S. Glass, N. E. Gruhn, E. Lorange, M. S. Singh, N. Y. T. Stessman, U. I. Zakai, *Inorg. Chem.* **2005**, 44, 5728.
- [8] a) M. K. Harb, T. Niksch, J. Windhager, H. Görls, R. Holze, L. T. Lockett, N. Okumura, D. H. Evans, R. S. Glass, D. L. Lichtenberger, M. El-khateeb, W. Weigand, *Organometallics* **2009**, 28, 1039; b) U.-P. Apfel, Y. Halpin, M. Gottschaldt, H. Görls, J. G. Vos, W. Weigand, *Eur. J. Inorg. Chem.* **2008**, 5112; c) L.-C. Song, B. Gai, H.-T. Wang, Q.-M. Hu, *J. Inorg. Biochem.* **2009**, 103, 805; d) M. K. Harb, U.-P.

¹⁾ CCDC-898493 (for **2**) and -898494 (for **3**) contain the supplementary crystallographic data for this paper (excluding structure factors). This data can be obtained free of charge via http://www.ccdc.cam.ac.uk/data_request/cif.

- Apfel, J. Kübel, H. Görls, G. A. N. Felton, T. Sakamoto, D. H. Evans, R. S. Glass, D. L. Lichtenberger, M. El-khateeb, W. Weigand, *Organometallics* **2009**, *28*, 6666; e) W. Gao, L.-C. Song, B.-S. Yin, H.-N. Zan, D.-F. Wang, H.-B. Song, *Organometallics* **2011**, *30*, 4097.
- [9] E. Block, E. V. Dikarev, R. S. Glass, J. Jin, B. Li, X. Li, S.-Z. Zhang, *J. Am. Chem. Soc.* **2006**, *128*, 14949.
- [10] H. K. Spencer, M. V. Lakshmikantham, M. P. Cava, *J. Am. Chem. Soc.* **1977**, *99*, 1470.
- [11] A. F. Hollemann, E. Wiberg, 'Lehrbuch der Anorganischen Chemie', 101th edn., Walter de Gruyter GmbH, Berlin–New York, 1995.
- [12] G. A. Kalabin, V. M. Bzehezovskii, D. F. Kushnarev, A. G. Proidakov, *J. Org. Chem. USSR* **1981**, *17*, 1009.
- [13] X. Zhao, I. P. Georgakaki, M. L. Miller, J. C. Yarbrough, M. Y. Darensbourg, *J. Am. Chem. Soc.* **2001**, *123*, 9710; X. Zhao, C.-Y. Chiang, M. L. Miller, M. V. Rampersad, M. Y. Darensbourg, *J. Am. Chem. Soc.* **2003**, *125*, 518; F. Gloaguen, J. D. Lawrence, M. Schmidt, S. R. Wilson, T. B. Rauchfuss, *J. Am. Chem. Soc.* **2001**, *123*, 12518; E. J. Lyon, I. P. Georgakaki, J. H. Reibenspies, M. Y. Darensbourg, *J. Am. Chem. Soc.* **2001**, *123*, 3268; J. D. Lawrence, H. Li, T. B. Rauchfuss, M. Bénard, M.-M. Rohmer, *Angew. Chem., Int. Ed.* **2001**, *40*, 1768; M. Razavet, S. C. Davies, D. L. Hughes, J. E. Barclay, D. J. Evans, S. A. Fairhurst, X. Liu, C. J. Pickett, *Dalton Trans.* **2003**, 586; R. C. Linck, T. B. Rauchfuss, *Bioorganometallics* **2006**, 403; H. Li, T. B. Rauchfuss, *J. Am. Chem. Soc.* **2002**, *124*, 726; S. Ott, M. Kritikos, B. Åkermark, L. Sun, *Angew. Chem., Int. Ed.* **2003**, *42*, 3285; C. Tard, X. Liu, S. K. Ibrahim, M. Bruschi, L. De Gioia, S. C. Davies, X. Yang, L.-S. Wang, G. Sawers, C. J. Pickett, *Nature (London, U.K.)* **2005**, 433, 610; L.-C. Song, Z.-Y. Yang, H.-Z. Bian, Q.-M. Hu, *Organometallics* **2004**, *23*, 3082; D. Seyferth, R. S. Henderson, L.-C. Song, *Organometallics* **1982**, *1*, 125; D. Seyferth, R. S. Henderson, L.-C. Song, *J. Organomet. Chem.* **1980**, *192*, C1; U. P. Apfel, Y. Halpin, H. Görls, J. G. Vos, B. Schweizer, G. Linti, W. Weigand, *Chem. Biodiversity* **2007**, *4*, 2138; J. Windhager, R. A. Seidel, U. P. Apfel, H. Görls, G. Linti, W. Weigand, *Eur. J. Inorg. Chem.* **2008**, 2023; J. Windhager, M. Rudolph, S. Bräutigam, H. Görls, W. Weigand, *Eur. J. Inorg. Chem.* **2007**, 2748; J. Windhager, H. Görls, H. Petzold, G. Mloston, G. Linti, W. Weigand, *Eur. J. Inorg. Chem.* **2007**, 4462; L.-C. Song, Z.-Y. Yang, H.-Z. Bian, Y. Liu, H.-T. Wang, X.-F. Liu, Q.-M. Hu, *Organometallics* **2005**, *24*, 6126.
- [14] G. A. N. Felton, C. A. Mebi, B. J. Petro, A. K. Vannucci, D. H. Evans, R. S. Glass, D. L. Lichtenberger, *J. Organomet. Chem.* **2009**, *694*, 2681.
- [15] R. C. Burns, M. J. Collins, R. J. Gillespie, G. J. Schrobilgen, *Inorg. Chem.* **1986**, *25*, 4465.
- [16] COLLECT, Data Collection Software, *Nonius B. V.*, Netherlands, 1998.
- [17] Z. Otwinowski, W. Minor, 'Processing of X-Ray Diffraction Data Collected in Oscillation Mode', in 'Methods in Enzymology', Vol. 276, 'Macromolecular Crystallography, Part A', Eds. C. W. Carter, R. M. Sweet, Academic Press, San Diego, CA, 1997, p. 307–326.
- [18] G. M. Sheldrick, *Acta Crystallogr., Sect. A* **2008**, *64*, 112.

Received August 8, 2012